Toxicology Letters 204 (2011) 71–80

Contents lists available at ScienceDirect

Toxicology Letters

journal homepage: www.elsevier.com/locate/toxlet

Involvement of oxidative stress-mediated ERK1/2 and p38 activation regulated mitochondria-dependent apoptotic signals in methylmercury-induced neuronal cell injury

Tien-Hui Lu[a,1], Shan-Yu Hsieh[b,1], Cheng-Chien Yen[c,d,1], Hsi-Chin Wu[e,1], Kuo-Liang Chen[e,1], Dong-Zong Hung[a,f], Chun-Hung Chen[a,g], Chin-Ching Wu[h], Yi-Chang Su[i], Ya-Wen Chen[j], Shing-Hwa Liu[k,*], Chun-Fa Huang[i,**]

[a] *Graduate Institute of Drug Safety, College of Pharmacy, China Medical University, Taichung 404, Taiwan*
[b] *School of Pharmacy, College of Pharmacy, China Medical University, Taichung 404, Taiwan*
[c] *Department of Occupational Safety and Health, College of Health Care and Management, Chung Shan Medical University, Taichung 402, Taiwan*
[d] *Department of Occupational Medicine, Chung Shan Medical University Hospital, Taichung 402, Taiwan*
[e] *Department of Urology, China Medical University Hospital, Taichung, Taiwan*
[f] *Toxicology Center, China Medical University Hospital, Taichung 404, Taiwan*
[g] *Department of Emergency, China Medical University Hospital, Taichung 404, Taiwan*
[h] *Department of Public Health, China Medical University, Taichung 404, Taiwan*
[i] *School of Chinese Medicine, College of Chinese Medicine, China Medical University, Taichung 404, Taiwan*
[j] *Department of Physiology, and Graduate Institute of Basic Medical Science, College of Medicine China Medical University, Taichung 404, Taiwan*
[k] *Institute of Toxicology, College of Medicine, National Taiwan University, Taipei 100, Taiwan*

ARTICLE INFO

Article history:
Received 3 January 2011
Received in revised form 16 April 2011
Accepted 18 April 2011
Available online 23 April 2011

Keywords:
Methylmercury
Neurotoxicity
Apoptosis
Oxidative stress
ERK1/2
p38

ABSTRACT

Methylmercury (MeHg) is well-known for causing irreversible damage in the central nervous system as well as a risk factor for inducing neuronal degeneration. However, the molecular mechanisms of MeHg-induced neurotoxicity remain unclear. Here, we investigated the effects and possible mechanisms of MeHg in the mouse cerebrum (*in vivo*) and in cultured Neuro-2a cells (*in vitro*). *In vivo* study showed that the levels of LPO in the plasma and cerebral cortex significantly increased after administration of MeHg (50 μg/kg/day) for 7 consecutive weeks. MeHg could also decrease glutathione level and increase the expressions of caspase-3, -7, and -9, accompanied by Bcl-2 down-regulation and up-regulation of Bax, Bak, and p53. Moreover, treatment of Neuro-2a cells with MeHg significantly reduced cell viability, increased oxidative stress damage, and induced several features of mitochondria-dependent apoptotic signals, including increased sub-G1 hypodiploids, mitochondrial dysfunctions, and the activation of PARP, and caspase cascades. These MeHg-induced apoptotic-related signals could be remarkably reversed by antioxidant NAC. MeHg also increased the phosphorylation of ERK1/2 and p38, but not JNK. Pharmacological inhibitors NAC, PD98059, and SB203580 attenuated MeHg-induced cytotoxicity, ERK1/2 and p38 activation, MMP loss, and caspase-3 activation in Neuro-2a cells. Taken together, these results suggest that the signals of ROS-mediated ERK1/2 and p38 activation regulated mitochondria-dependent apoptotic pathways that are involved in MeHg-induced neurotoxicity.

Abbreviations: LPO, lipid peroxidation; PARP, poly (ADP-ribose) polymerase; NAC, *N*-acetylcysteine; MAPKs, mitogen-activated protein kinases; ERK, extracellular signal-regulated kinases; JNK, c-Jun N-terminal kinases; MMP, mitochondrial membrane potential; ROS, reactive oxygen species; GSH, glutathione.

* Corresponding author at: Institute of Toxicology, College of Medicine, National Taiwan University, No. 1, Section 1, Jen-Ai Road, Taipei 100, Taiwan. Tel.: +886 2 23123456x88605; fax: +886 2 23410217.
** Corresponding author at: School of Chinese Medicine, College of Chinese Medicine, China Medical University, No. 91 Hsueh-Shih Road, Taichung 404, Taiwan. Tel.: +886 4 22053366x3323; fax: +886 4 22333641.
E-mail addresses: shliu@ha.mc.ntu.edu.tw (S.-H. Liu), cfhuang@mail.cmu.edu.tw (C.-F. Huang).
[1] These authors contributed equally to this work.

0378-4274/$ – see front matter © 2011 Elsevier Ireland Ltd. All rights reserved.
doi:10.1016/j.toxlet.2011.04.013

1. Introduction

Methylmercury (MeHg) is a highly lipophilic and toxic environmental contaminant. It has become an important public health problem in humans because of the growing evidence of its contamination of the human food chain, such as in fish, shellfish, and other aquatic mammals (Clarkson et al., 2003; U.S. Environmental Protection Agency (EPA, 1997). MeHg, which easily crosses the blood–brain barrier (BBB), is a potent neurotoxin interfering with the brain and nervous system (the primary target tissue for the toxic effects of MeHg), and causes irreversible neuropathophysiological disorders in mammals (Li et al., 2010; Rice and Barone, 2000). It has been clinically reported that after the MeHg disasters in Japan and Iraq, adults as well as infants and children developed severe brain dysfunction and damage (Amin-Zaki et al., 1981; Marsh, 1987). Although a previous study by our group indicated that exposure of mice to MeHg, which may be similar to the dose by ingestion in MeHg-contaminated areas, could cause abnormal neural function (Huang et al., 2008), the signaling mechanisms of MeHg-induced neurotoxic effects are not yet understood.

Oxidative stress has been implicated in a wide variety of biological reactions such as cell death or central nervous system damage (Cuello et al., 2010; Tamm et al., 2006). Exposure to MeHg (1–10 μM) has been reported to induce toxic effects by production of oxidative stress, which alters cellular function and eventually results in pathophysiological injury and cell death in various cells, including neuronal cells (Garg and Chang, 2006; Yin et al., 2007). Some studies have also indicated that MeHg disrupts cellular redox homeostasis and/or antioxidant enzymes and the mitochondrial electron transport chain, via excessive generation of ROS (Sarafian, 1999; Yee and Choi, 1996), thus reducing the mitochondrial inner membrane potential by altering calcium homeostasis (Levesque and Atchison, 1991; Sirois and Atchison, 2000). Moreover, MeHg-induced oxidative stress can inhibit glutamate uptake of astrocytes, while stimulating glutamate over efflux, which results in an excessive level of synaptic glutamate and disrupts glutamine/glutamate cycling (Aschner et al., 2007; Yin et al., 2007). These undesirable MeHg-induced biological processes ultimately lead to neuronal dysfunction and cell death and suggest an association with progressive neurodegenerative diseases (Larkfors et al., 1991; Mutter et al., 2007).

Mitogen-activated protein kinases (MAPKs) are a family of serine/threonine protein kinases that mediate a critical role of signal transduction in mammals. MAPKs, which can be subdivided into ERK1/2, JNK, and p38 protein, are activated by modulation of important cellular functions, including proliferation, differentiation, or response to environmental stimuli such as apoptosis (Chang and Karin, 2001; Cowan and Storey, 2003). It has been proposed that deviation from the precise regulation of MAPK signaling pathways could cause the development of human neurodegenerative diseases (Kim and Choi, 2010). ROS-induced oxidative stress has been demonstrated to activate members of the MAPKs via phosphorylation (El-Najjar et al., 2010; Navarro et al., 2006), and it is also implicated in cellular injuries or apoptosis during neurodegenerative disorders (Loh et al., 2006). Recently, oxidative stress-induced ERK/p38 activation has been identified in mammalian cell deaths caused by exposure to toxic chemicals (Martin and Pognonec, 2010; Navarro et al., 2006). However, the mechanism underlying the effect of MeHg-induced oxidative stress in neuronal cells contributing to apoptosis is not clear.

In this study, we attempted to explore the role of oxidative stress-mediated signaling in neuronal cell death by investigating whether ROS generation, mitochondrial dysfunction, caspase cascades, and ERK/p38-MAPK activation are involved in MeHg-induced apoptosis in Neuro-2a cells. Moreover, the use of the potent antioxidant *N*-acetylcysteine (NAC) at different stages confirmed the involvement of major molecules in signaling pathways. We also explored whether exposure to MeHg (50 μg/kg), which mimics the possible exposure dose in humans in MeHg-contaminated areas, and has been reported to cause the neurophysiological dysfunction (Huang et al., 2008), would generate LPO, deplete GSH levels, and alter apoptotic-related gene expressions in the cerebral cortex of mice.

2. Materials and methods

2.1. Cell culture

Murine neuroblastoma cell line: Neuro-2a (CCL-131, American Type Culture Collection, Manassas, VA, USA) was cultured in a humidified chamber with a 5% CO_2–95% air mixture at 37 °C and maintained in Dulbecco's modified Eagle's medium (DMEM) supplemented with 10% fetal bovine serum (FBS) and 1% penicillin–streptomycin (Gibco/Invitrogen, Carlsbad, CA, USA), and all assays were conducted within 10–15 cell passages after unfreezing the cells from the liquid nitrogen (to keep the best morphological and biological characteristics).

2.2. Cell viability

Neuro-2a cells were seeded at 2×10^4 cells/well in 96-well plates and allowed to adhere and recover overnight. The cells were transferred to fresh media and then incubated with MeHg (1–5 μM; Sigma-Aldrich, St. Louis, MO, USA) in the absence or presence of NAC (1 mM) or specific MAPK inhibitors (20 μM, Sigma-Aldrich) for 24 h. After incubation, the medium was aspirated and fresh medium containing 30 μL of 2 mg/mL 3-(4, 5-dimethyl thiazol-2-yl-)-2, 5-diphenyl tetrazolium bromide (MTT; Sigma-Aldrich) was added. After 4 h, the medium was removed and replaced with blue formazan crystal dissolved in dimethyl sulfoxide (100 μL; Sigma-Aldrich). Absorbance at 570 nm was measured using a microplate reader (Bio-Rad, model 550, Hercules, CA, USA).

2.3. Determination of reactive oxygen species (ROS) production

ROS generation was monitored by flow cytometry using the peroxide-sensitive fluorescent probe: 2′,7′-dichlorofluorescein diacetate (DCFH-DA, Molecular Probes, Inc., Eugene, OR, USA), as described by Chen et al. (2010). In brief, cells were coincubated with 20 μM DCFH-DA at 37 °C. After incubation with the dye, cells were resuspended in ice-cold phosphate buffered saline (PBS) and placed on ice in a dark environment. The intracellular peroxide levels were measured by flow cytometer (FACScalibur, Becton Dickinson, Sunnyvale, CA), which emitted a fluorescent signal at 525 nm. Each group was acquired with more than 10,000 individual cells.

2.4. Analysis of intracellular GSH contents

Neuro-2a cells were seeded at 2×10^5 cells/well in a 24-well plate and allowed to adhere and recover overnight. The cells were transferred to fresh media and incubated with MeHg in the absence or presence of NAC (1 mM, Sigma-Aldrich) for 24 h. Then, cells were washed twice with PBS, and then a new medium which contained 60 μM monochlorobimane (mBCL, a sensitive fluorescent probe, Sigma-Aldrich) was added and incubated for further 30 min at 37 °C. After loading the culture cells with mBCL, the supernatants were discarded, cells were washed twice with PBS, and the measurement of the intracellular GSH levels was performed as described previously (Yen et al., 2007).

2.5. Flow cytometric analysis of sub-G1 DNA content

Cells were seeded (in the same manner as for intracellular GSH analysis) and incubated with MeHg. After 24 h incubation, the cells were detached, collected, and washed with PBS, and the analysis of sub-G1 DNA content was performed as described previously (Lu et al., 2011). The cells were subjected to flow cytometry analysis of DNA content (FACScalibur, Becton Dickinson). Nuclei displaying hypodiploid, sub-G1 DNA contents were identified as apoptotic. The sample of each group was collected with more than 10,000 individual cells.

2.6. Determination of mitochondrial membrane potential (MMP)

Cells were seeded (in the same manner as for intracellular GSH analysis) and exposed to MeHg in the absence or presence of NAC (1 mM) or specific MAPK inhibitors (20 μM, Sigma-Aldrich). After 6 h or 24 h incubation, cells were loaded with 100 nM 3,3′-di-hexyloxacarbocyanine iodide ($DiOC_6$, Molecular Probes, Inc.) for 30 min at 37 °C, and then trypsinized, collected, and washed twice with PBS. MMP was analyzed by FACScan flow cytometer (excitation at 475 nm and emission at 525 nm, Becton Dickinson) (Chen et al., 2006).

2.7. Measurement of caspase-3 activity

Neuro-2a cells were seeded (in the same manner as for intracellular GSH analysis) and exposed to MeHg in the absence or presence of NAC (1 mM, Sigma-Aldrich) or specific MAPK inhibitors (20 μM, Sigma-Aldrich). After 24 h incubation, the cells were lysed and caspase-3 activity was determined using the CaspACE™ fluorometric activity assay (Promega Corporation, Madison, WI, USA) as previously described (Lu et al., 2011). Protein levels of cell lysate samples were determined using the bicinchoninic acid protein assay kit with an absorption band of 570 nm (Pierce, Rockford, IL, USA) to normalize the cell numbers between control and different MeHg-treated groups.

2.8. Western blot analysis

Neuro-2a cells were seeded at 1×10^6 cells/well in a 6-well plate and allowed to adhere and recover overnight. The cells were transferred to fresh media and incubated with MeHg in the absence or presence of NAC (1 mM, Sigma-Aldrich) or specific MAPK inhibitors (20 μM, Sigma-Aldrich) for different time intervals. After treatment, the expression of protein activation or phosphorylation was evaluated by the standard protocol performance of Western blot (as previously described in Chen et al., 2010) using the specific antibodies, including: anti-cleaved caspase-3, -7, and -9, PARP, phosphor-p38 and phosphor-ERK1/2 (Cell Signaling Technology, Inc., Beverly, MA, USA), anti-Bcl-2, Bax, p38, and ERK1/2 (Santa Cruz Biotechnology, Inc., CA, USA), and α-tubulin (Epitomics, Inc., Burlingame, CA, USA).

2.9. Animal preparation

Randomly bred, normal male ICR mice (4 weeks old, 20–25 g) were obtained from the Animal Center of College of Medical, National Taiwan University. All experiments were carried out according to the protocols approved by the Institutional Animal Care and Use Committee (IACUC), and the care and use of laboratory animals were conducted in accordance with the guidelines of the Animal Research Committee of China Medical University (http://cmurdc.cmu.edu.tw/LA/index.php). Mice were randomly assigned to pretreatment groups, weighed, and administered MeHg or vehicle (oral application by gavage). These groups were given 0 and 50 μg/kg/day MeHg in the absence or presence of NAC (150 mg/kg/day) for 7 consecutive weeks. Each group contained more than 12 mice ($n = 12–15$). All experimental mice were subject to deep anesthesia by an intraperitoneal injection of pentobarbital (80 mg/kg) and the whole blood samples were collected from an eyehole vessel. Whole blood sample were centrifuged at $3000 \times g$ for 10 min, plasma was obtained, and LPO levels were assayed immediately. At the same time, mice were sacrificed by decapitation under pentobarbital anesthesia, the cerebral cortex was quickly removed and stored in liquid nitrogen until use, and then the analysis of LPO levels, GSH content, and apoptosis-related gene expression was performed.

2.10. Lipid peroxidation (LPO) analysis

Neuro-2a cells were seeded (in the same manner as for Western blot analysis) and exposed to MeHg alone or in combination with NAC (1 mM, Sigma-Aldrich). After 24 h incubation, cells were harvested and homogenized in ice-cold 20 mM Tris–HCl buffer, pH 7.4, containing 0.5 mM butylated hydroxytoluene to prevent sample oxidation. The cerebral cortex was weighed and homogenized separately in ice-cold 20 mM Tris–HCl buffer, pH 7.4 (100 mg tissue/mL buffer), then homogenized sample was assayed immediately. LPO levels of equal volumes of sample were measured using a commercial LPO assay kit (Calbiochem, La Jolla, CA, USA) as described by Huang et al. (2008) and Lu et al. (2010). The protein concentration of each sample was determined using the bicinchoninic acid protein assay kit (Pierce). LPO level was expressed as nanomoles (nmol) MDA per milligram protein and estimated from the standard curve.

2.11. Measurement of glutathione (GSH) levels in the cerebral cortex

The cerebral cortex was homogenized with an isotonic buffer (25 mM Hepes, pH 7.4, containing 250 mM sucrose) and then centrifuged at $1000 \times g$ at 4 °C. The pellet for each sample was discarded, 10× lysis buffer was added to the supernatant, and it was placed on ice for 10 min. After centrifugation, the supernatant was performed the measurement of GSH levels using glutathione assay kit (Sigma-Aldrich) according to the manufacturer's instructions. The protein concentration of each sample was determined using the bicinchoninic acid protein assay kit (Pierce). GSH level was expressed as nanomoles (nmol) GSH per microgram protein and estimated from the standard curve.

2.12. Real-time quantitative reverse-transcribed polymerase chain reaction (RT-PCR) analysis

The expression of apoptosis-related genes was evaluated by real-time quantitative RT-PCR, as previously described (Lu et al., 2010). Briefly, intracellular total RNA was extracted from the cerebral cortex using RNeasy kits (Qiagen, Hilden, Germany) and reverse transcribed into cDNA using the AMV RTase (reverse transcriptase enzyme; Promega Corporation, Pty. Ltd.) according to the manufacturer's instructions. Each sample (2 μL cDNA) was tested with real-time Sybr Green PCR reagent (Invitrogen, USA) with mouse specific primers (PCR primers for the examined genes were listed in Table 1) in a 25-μL reaction volume, and amplification was performed using an ABI StepOnePlus sequence detection system (PE, Applied Biosystems, CA, USA). Data analysis was performed using StepOne™ software (Version 2.1, Applied Biosystems). All amplification curves were analyzed with a normalized reporter (R_n: the ratio of the fluorescence emission intensity to the fluorescence signal of the passive reference dye) threshold of 0.2 to obtain the C_T values (threshold cycle). The reference control genes were measured with four replicates in each PCR run, and their average C_T was used for relative quantification analyses (the relative quantification method utilizing real-time PCR efficiencies (Pfaffl et al., 2002)). TF expression data were normalized by subtracting the mean of reference gene C_T value from their C_T value (ΔC_T). The fold change value was calculated using the expression $2^{-\Delta\Delta C_T}$, where $\Delta\Delta C_T$ represents $\Delta C_{T\text{-condition of interest}} - \Delta C_{T\text{-control}}$. Prior to conducting statistical analyses, the fold change from the mean of the control group was calculated for each individual sample.

2.13. Statistical analysis

Data are presented as means ± standard deviations (S.D.). The significance of difference was evaluated by the Student's *t*-test. When more than one group was compared with one control, significance was evaluated according to one-way analysis of variance (ANOVA), and the Duncan's post hoc test was applied to identify group differences. The *p* value less than 0.05 was considered to be significant. The statistical package SPSS, version 11.0 for Windows (SPSS Inc., Chicago, IL, USA) was used for the statistical analysis.

3. Results

3.1. MeHg exposure induces LPO production, depletion of GSH levels, and changes in apoptosis-related gene expression in the cerebral cortex of mice

Our previous study indicated that exposure to MeHg (50 μg/kg/day) caused neurophysiological dysfunctions and biological changes in mice brain, accompanied by significant mercury accumulation (Huang et al., 2008). However, the toxicological effects and possibly molecular mechanism of MeHg-induced neurotoxicity have not been understood. Therefore, we investigated the LPO and GSH levels in the plasma and/or cerebral cortex of MeHg-treated mice (50 μg/kg/day, by oral gavage). The results revealed that LPO levels in the plasma and cerebral cortex significantly increased after MeHg exposure for 7 consecutive weeks (Supplement Fig. 1), whereas the GSH levels in the cerebral cortex markedly decreased (Fig. 1).

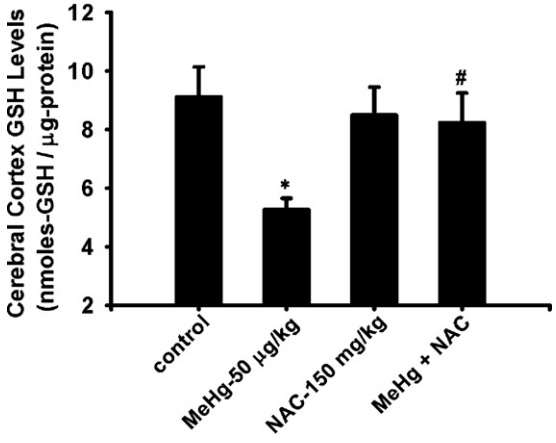

Fig. 1. Influence of MeHg on GSH levels of cerebral cortex in MeHg-exposed mice. The GSH levels in the cerebral cortex of mice treated with MeHg (50 μg/kg/day) for 7 consecutive weeks in the absence or presence of NAC (150 mg/kg/day) was detected as described in Section 2. All data are presented as mean ± S.D. ($n = 12–15$ for each group). $^*p < 0.05$ as compared with vehicle control group. $^\#p < 0.05$ as compared with MeHg group alone.

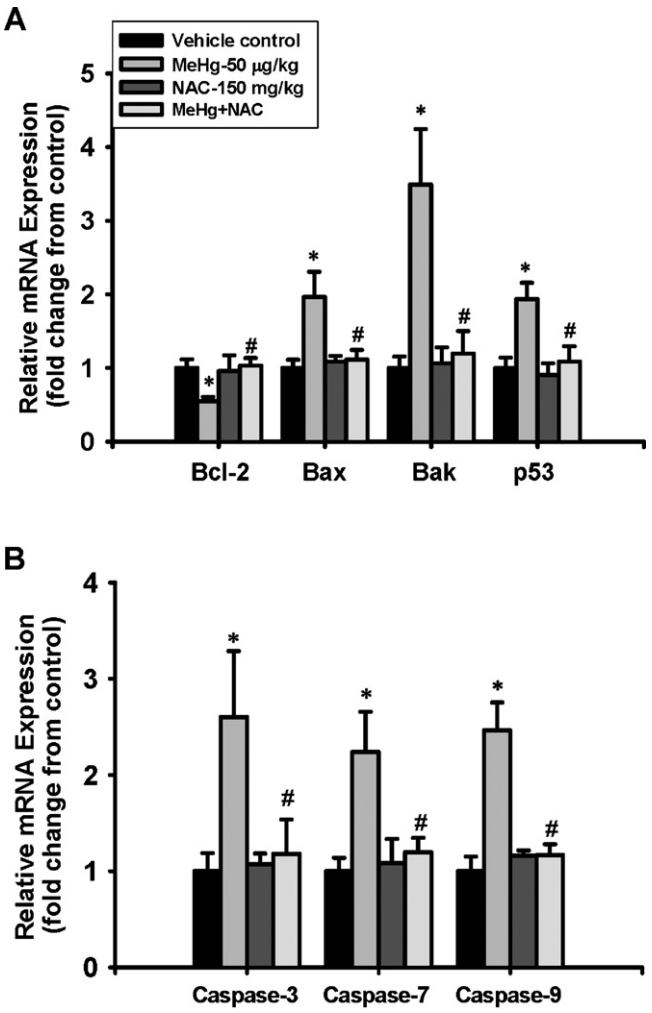

Fig. 2. MeHg treatment regulated gene expression for apoptotic factors in the cerebral cortex of mice. Mice were treated with MeHg (50 μg/kg/day) for 7 consecutive weeks in the absence or presence of NAC (150 mg/kg/day), and the expression of anti-apoptotic (Bcl-2) and pro-apoptotic (Bax, Bak, p53) (A), and caspase-related genes (caspase-3, -7, and -9) (B) of the cerebral cortex was analyzed by real-time quantitative RT-PCR using SYBR Green. Target gene expression was normalized toβ-actin, and the results are expressed as fold change from vehicle control. Results are expressed as mean ± S.D. (n = 12–15 for each group). $^{*}p < 0.05$ as compared with vehicle control group. $^{\#}p < 0.05$ as compared with MeHg group alone.

We further investigated whether MeHg-induced oxidative stress could cause apoptosis in the cerebral cortex of mice. To address this issue, we analyzed apoptosis-related gene expression by using real-time quantitative RT-PCR. As shown in Fig. 2, there were significant down-regulation of Bcl-2 (anti-apoptotic gene) and up-regulation of Bax, Bak, and p53 (pro-apoptotic genes) expressions in the cerebral cortex of mice after MeHg exposure for 7 consecutive weeks (Fig. 2A). Furthermore, these changes were accompanied by marked up-regulation of caspase-3, -7, and -9 expressions (Fig. 2B). Antioxidant NAC (150 mg/kg/day) effectively prevented MeHg-induced toxic responses (Supplement Fig. 1, Figs. 1 and 2).

3.2. MeHg induces cell death, ROS production, and intracellular GSH depletion in Neuro-2a cells

To investigate whether the mechanisms involved in MeHg-induced neurotoxicity, we explored the *in vitro* effects of MeHg in Neuro-2a cells. The cell viability of Neuro-2a cells was markedly decreased after 24 h MeHg (1–5 μM) treatment, and the LD_{50} was determined to be approximately 3 μM (Fig. 3A).

To further evaluate the effects of MeHg on oxidative stress damage, we treated the cells with MeHg (3 and 5 μM) and measured ROS generation, LPO production, and intracellular GSH levels. After exposure of Neuro-2a cells to MeHg for 0.5–2 h, the intracellular ROS levels were found to be significantly increased by using DCF fluorescence probe as an indicator of ROS formation (Fig. 3B). Incubation of cells with MeHg for 24 h also produced remarkably high malondialdehyde (MDA) levels in the cell membrane (3 μM MeHg, 3.08 ± 0.07; 5 μM MeHg, 3.91 ± 0.08; control, 1.92 ± 0.08 nmol MDA/mg protein) (Fig. 3C). Moreover, the levels of intracellular GSH (a principal cellular protective thiol against oxidative stress-induced toxicity, and determined using an mBCL fluorescent probe) were significantly decreased after treatment with MeHg (3 and 5 μM, not 1 μM) for 24 h (3 μM MeHg, 61.31 ± 3.13%; 5 μM MeHg, 30.60 ± 4.07% of control) (Fig. 3D). These MeHg-induced responses could be reversed by NAC (1 mM) (Fig. 3B–E).

3.3. MeHg causes cell death via mitochondria-dependent apoptosis pathways in Neuro-2a cells

To investigate the involvement of apoptosis in MeHg-induced Neuro-2a cell cytotoxicity, we analyzed the sub-G1 hypodiploid cell population (as an indicator of apoptosis) by flow cytometry. Cells treated with MeHg (3 and 5 μM) for 24 h exhibited a significant increase in the sub-G1 hypodiploid cell population (Fig. 4A). Moreover, caspase-3 activity (an integral step in the majority of apoptotic events) was also markedly induced after treatment of Neuro-2a cells with MeHg (Fig. 4B). These results indicated that exposure of Neuro-2a cells to MeHg could induce apoptosis.

Next, we explored whether MeHg-induced apoptosis mediated through mitochondrial dysfunction. To show that MeHg affected mitochondrial permeability transition, MMP was analyzed using flow cytometry with the cationic dye $DiOC_6$. As shown in Fig. 5A, exposure of Neuro-2a cells to MeHg (3 μM) markedly induced MMP loss (for 6 and 24 h). We also investigated cytochrome *c* release from the mitochondria into the cytosol in MeHg-treated Neuro-2a cells. Cells exposure to MeHg (3 μM) for 6 h effectively increased cytochrome *c* release in the cytosol fraction, and this increase in the level of cytochrome *c* was more significant after 24 h MeHg exposure (Fig. 5B). Antioxidant NAC (1 mM) could effectively

Table 1
Primer sequences used for the real-time quantitative RT-PCR analysis.

Gene	Forward (5′ → 3′)	Reverse (5′ → 3′)	Reference
Bcl-2	TGGTCTCTATTGCAGCTCAGAC	TGGCCCAATCTAGGAAATGTTC	Harvilchuck and Carlson (2009)
Bax	GGAATTCCAAGAAGCTGAGCGAGTGT	GGAATTCTTCTTCCAGATGGTGAGCGAG	Hoijman et al. (2004)
Bak	CCCAGGACACAGAGGAGGTC	GCCCAACAGAACCACACCAAAA	Kim et al. (2004)
p53	GGGACAGCCAAGTCTGTTATG	GGAGTCTTCCAGTGT GATAT	Kalia and Bansal (2009)
Caspase-3	GGAGCTGGACTGTGGCATTGA	CAGTTCTTTCGTGAGCATGGA	Wang and Han (2009)
Caspase-7	CCGAGTGCCCACTTATCTGT	ACCTGTCGCTTTGTCGAAGT	Yang et al. (2008)
Caspase-9	TGCACTTCCTCTCAAGGCAGGACC	TCCAAGGTCTCCATGTACCAGGAGC	Kalia and Bansal (2009)
β-Actin	TGTGATGGTGGGAATGGGTCAG	TTTGATGTCACGCACGATTTCC	Min et al. (2009)

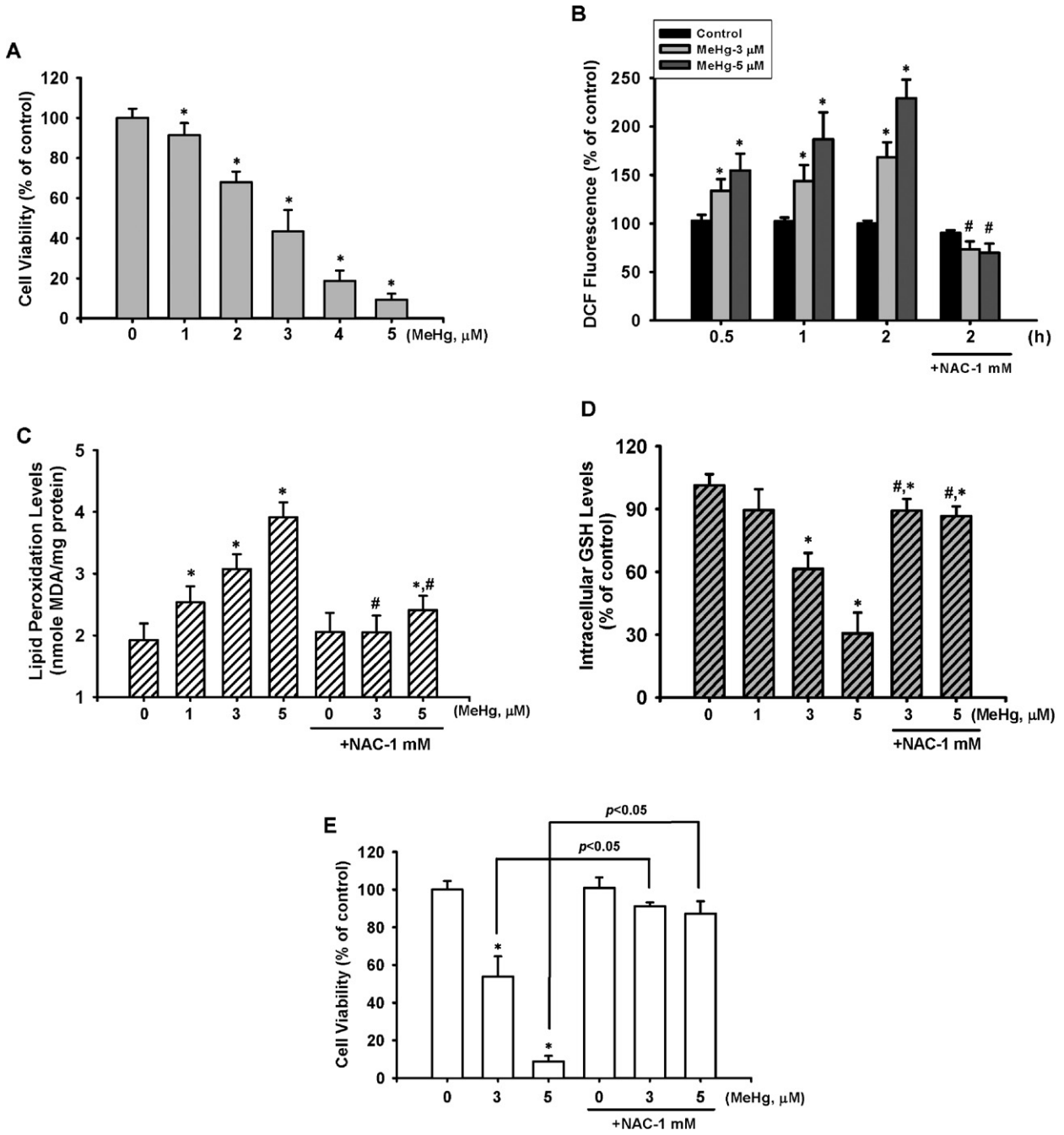

Fig. 3. Effects of MeHg on cell viability and oxidative stress damage generation in Neuro-2a cells. (A) Cells were incubated with MeHg (1–5 μM) for 24 h, and cell viability was determined by MTT assay. (B) Neuro-2a cells were incubated with MeHg (3 and 5 μM) for various time courses in the absence or presence of NAC (1 mM) for 2 h, and ROS was determined by flow cytometric analysis. (C) Cell membrane LPO production, (D) intracellular GSH levels, and (E) cell viability after incubation of Neuro-2a cells with MeHg (3 and 5 μM) for 24 h in the absence or presence of NAC (1 mM) were determined as described in Section 2. All data are expressed as mean ± S.D. for four independent experiments with triplicate determination. $^{*}p < 0.05$ as compared with vehicle control. $^{\#}p < 0.05$ as compared with MeHg alone.

reverse the MeHg-induced responses (Fig. 5A and B). Moreover, we further examined the changes in the expression of Bcl-2 family proteins. Treatment of Neuro-2a cells with MeHg (3 μM) significantly decreased the expression of Bcl-2 and increased the level of Bax, which led to a marked shift in the pro-apoptotic (Bax)/anti-apoptotic (Bcl-2) expression ratio toward an apoptosis-associated state (Fig. 5C).

To further investigate whether MeHg-induced the activation of cysteine proteases, which are important biomarkers of the apoptotic process representing both the initiation and execution of cell death, the expressions of caspase cascades were detected by Western blot analysis. As shown in Fig. 5D, it increased the activation of caspase-3 and -7 in Neuro-2a cells treated with MeHg (3 μM) for 6–24 h. The MeHg-induced caspase-3 activity in Neuro-2a cells could be reversed by NAC (Fig. 4B). MeHg also significantly increased the level of cleaved product (active form) of PARP as well as the expression of upstream caspase-9 (Fig. 5D).

3.4. Effects of MeHg on activation of ERK- and p38-MAPK in Neuro-2a cells

To further evaluate the involvement of MAPK signals in responses triggered by MeHg-induced apoptosis, the expressions of MAPK activation were examined. As shown in Fig. 6A, exposure

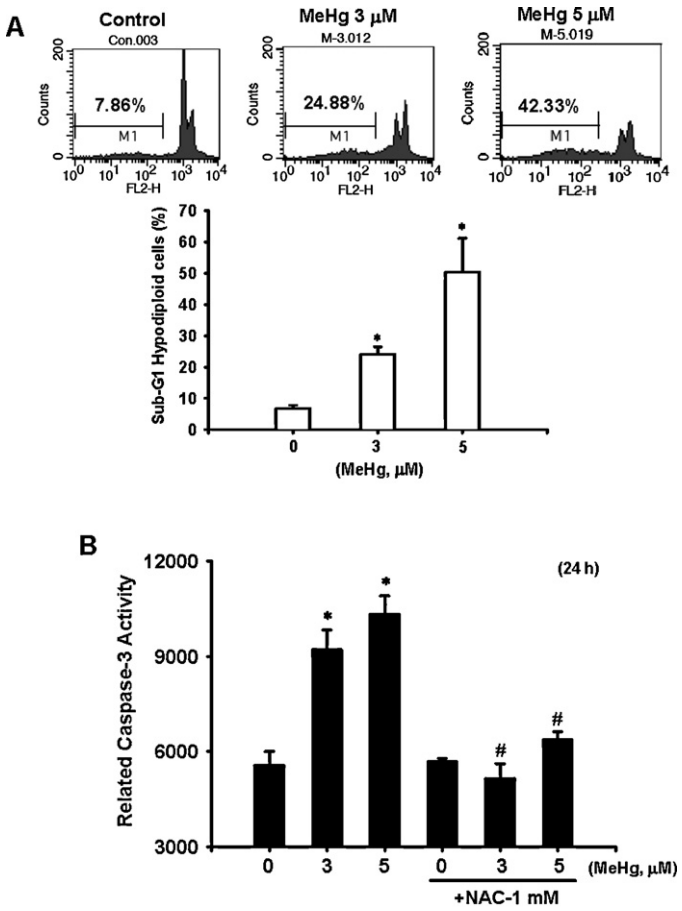

Fig. 4. Analysis of sub-G1 hypodiploid cell population and caspase-3 activity showing MeHg-induced apoptosis in Neuro-2a cells. Cells were incubated with MeHg (3 and 5 μM) for 24 h in the absence or presence of NAC (1 mM). (A) Cells with genomic DNA fragmentation (sub-G1 DNA content) were analyzed by flow cytometry, and (B) caspase-3 activity was measured by the CaspACE™ fluorometric activity assay kit as described in Section 2. Data are presented as mean ± S.D. for four independent experiments with triplicate determination. $^{*}p < 0.05$ as compared with vehicle control. $^{\#}p < 0.05$ as compared with MeHg group alone.

of Neuro-2a cells to MeHg (3 μM) significantly increased the levels of phosphorylation of ERK1/2- and p38-MAPK (for 0.5–2 h), but not that of JNK. To determine the relationship between MeHg-induced apoptotic signaling transduction in Neuro-2a cells and MAPK activation, the cells were pretreated with the specific ERK inhibitor PD98059, p38 inhibitor SB203580, and JNK inhibitor SP600125 for 1 h, and then incubated with MeHg (3 mM) for 24 h. It was found that MeHg-induced neuronal cell cytotoxicity was attenuated by the ERK1/2 and p38 inhibitors (20 μM), but not by the JNK inhibitor (Fig. 6B, a). NAC, ERK and p38 inhibitors could prevent MeHg-induced ERK1/2- and p38-MAPK activation (Fig. 6B, b and c). Loss of MMP and the increase of caspase-3 activity induced by MeHg-treated Neuro-2a cells could also be effectively reversed by ERK and p38 inhibitors (Fig. 6C and D). Furthermore, MeHg-induced increase in ERK1/2- and p38-MAPK protein phosphorylation was observed in the cerebral cortex of MeHg-treated mice (50 μg/kg/day, for 7 consecutive weeks), which could be prevented by NAC (Supplement Fig. 2). These results indicate that ROS-mediated ERK1/2 and p38-MAPK activation plays a crucial role in MeHg-induced neuronal cell apoptosis.

4. Discussion

Many studies have indicated that MeHg is a potent neurotoxicant affecting both the developing and mature central nervous system, and can cause severe neuropathophysiological disorders with exposure to high concentrations (0.5–40 ppm in drinking water or 0.2–2 mg/kg/day, for more than 7 consecutive days) in *in vivo* system, including loss of neurons in the calcarine cortex, cerebellar Purkinje, and granule cells, leading to vision, motion, or postural abnormalities (Carvalho et al., 2007; Chuu et al., 2007; Dare et al., 2003; Goulet et al., 2003; Onishchenko et al., 2007). It has also been reported that exposure to MeHg (20–50 μg/kg) in mice, which was the possible dosage from food ingested in MeHg-contaminated areas (8.03–174 μg MeHg/kg, even more than 200 μg MeHg/kg), caused severe neurotoxic injuries, accompanied by significant mercury accumulation (113.0–241.8 ng mercury/g wet. wt.) and oxidative stress generation in the brain regains (Grandjean et al., 1992; Huang et al., 2008, 2011; Maramba et al., 2006; Qiu et al., 2008). Oxidative stress, which has been demonstrated to strongly induce under MeHg-exposed conditions and play a key role in cascade activation during mercury-induced injury, is involved in the progression of brain and/or neuronal cell dysfunction and death in mammals (Dreiem et al., 2005; Shanker et al., 2004; Yin et al., 2007). Of late, an increasing number of studies have suggested that oxidative stress, which disturbs the physiological functions of neuronal cells and causes apoptosis, is linked to the progression of neurodegenerative diseases (Barnham et al., 2004; Loh et al., 2006), and clinical studies also described that significant and higher concentrations of mercury are detected in the blood and/or brain regions of Alzheimer's disease patients compared to healthy people; these suggest a decisive role of mercury in the origin or progression of neurodegenerative diseases (Gerhardsson et al., 2008; Hock et al., 1998; Mutter et al., 2007). Despite several studies showing that MeHg can produce neurotoxic injuries by inducing oxidative stress in mammals, the role of ROS and the precise signaling mechanisms underlying MeHg-induced neuronal degeneration and cell death are still unclear. In this study, our results revealed that MeHg significantly induced LPO production (as an indicator for oxidative stress damage formation) in the plasma and cerebral cortex of mice exposed to MeHg (50 μg/kg/day) for 7 consecutive weeks, which was accompanied by GSH depletion. Meanwhile, the results also revealed that MeHg significantly altered apoptosis-related gene expressions, including anti-apoptotic (Bcl-2), pro-apoptotic (Bax, Bak, and p53), and caspase cascades (caspase-3, -7, and -9) in the cerebral cortex of MeHg-treated mice. Moreover, MeHg (1–5 μM) exposure significantly decreased cell viability, increased ROS production, depleted intracellular GSH, and caused apoptotic events (increase in sub-G1 hypodiploid cell population and caspase cascade activation) in Neuro-2a cells. The antioxidant NAC could effectively prevent, but not fully reverse, these MeHg-induced responses. These findings indicate that oxidative stress is caused by MeHg exposure, and it may be involved in MeHg-induced neuronal degeneration and cell apoptosis. Furthermore, Fujimura et al. (2009) has reported that the expression of Rac1 (Rho-family protein) can be down-regulated and ultimately lead to apoptosis in MeHg-exposed neuronal cells. Tofighi et al. (2011) has also indicated that MeHg induces caspase-independent cell death via parallel activation of calpains and lysosomal proteases in hippocampal neurons. However, the critical roles of these signals in MeHg-induced neurotoxicity still require investigation in the future.

ROS can elicit oxidative stress, which triggers cell death; thus, it can be implicated in various neurodegenerative conditions resulting from metal-induced neurotoxicity (Bush, 2000; Rana, 2008). ROS is also known to cause mitochondrial dysfunction (being a key mechanism in apoptosis) by oxidative stress-induced apoptosis (Chen et al., 2006; Lu et al., 2011). Mitochondria are highly sensitive to the effects of oxidative stress, and 2 major events have been noted in oxidative stress-induced apoptosis involving mitochondrial dysfunction. One of the events is alteration in

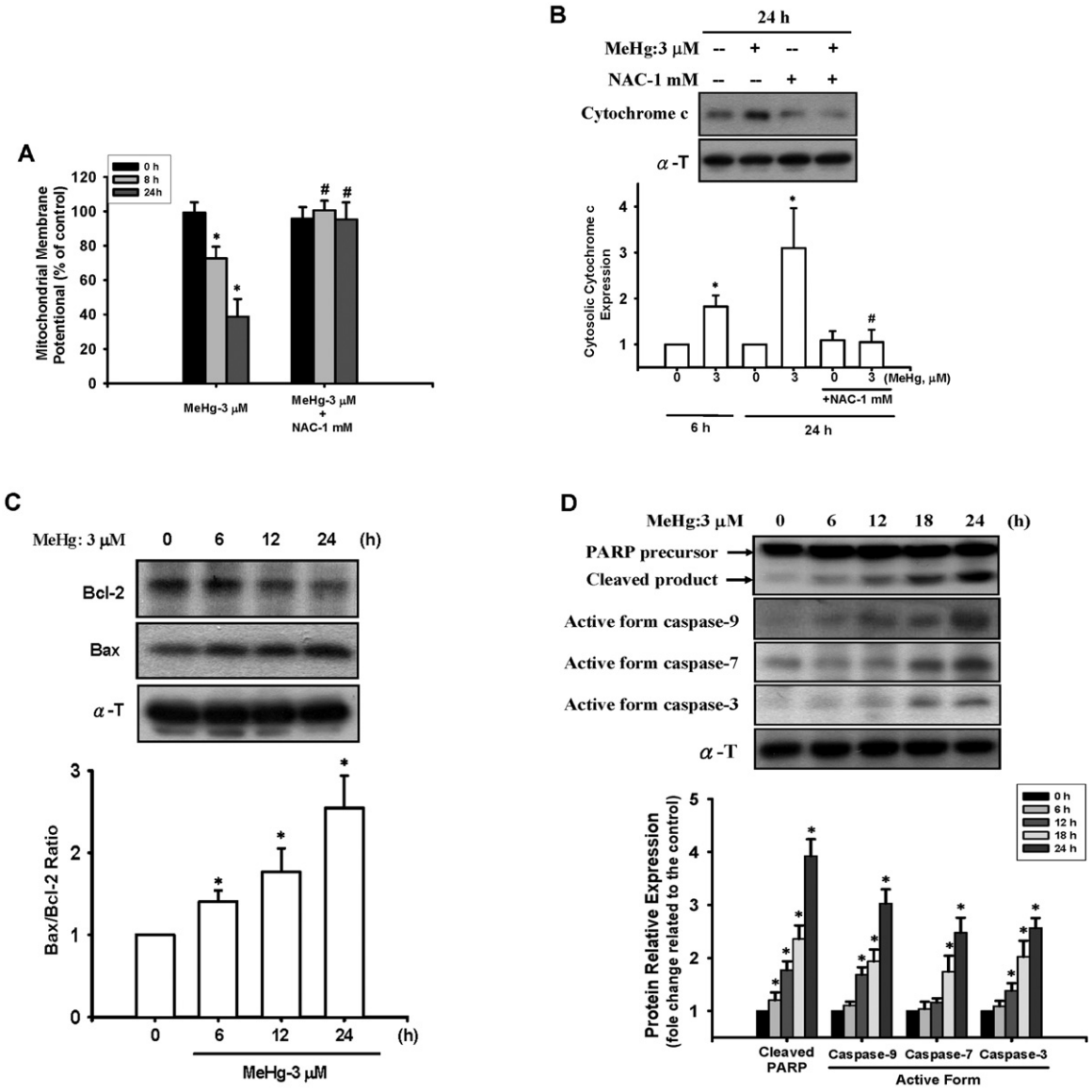

Fig. 5. MeHg induced mitochondrial dysfunction, cleavage of PARP, and caspase cascade activation in Neuro-2a cells. Cells were incubated with MeHg (3 μM or 5 μM) for 6–24 h in the absence or presence of NAC (1 mM). MMP depolarization was determined by flow cytometry (A); cytochrome *c* release (B), Bcl-2 and Bax protein expression (C), and PARP cleavage and the caspase-3, -7, and -9 expression (D) were examined by Western blot analysis as described in Section 2. Data in A are presented as mean ± S.D. for four independent experiments with triplicate determination. Results shown in B–D are typical representatives of at least three independent experiments. The intensity of bands was analyzed by densitometry and expressed as fold changes relative to the control (mean ± S.D.). $^{*}p < 0.05$ as compared with vehicle control. $^{\#}p < 0.05$ as compared with MeHg alone.

the mitochondrial membrane permeability and the subsequent depolarization of MMP; while the other event is the release of mitochondria-associated proteins (including cytochrome *c*, Apaf-1, and apoptosis-inducing factor) from the intermembrane space of mitochondria into the cytosol (Chen et al., 2010; Kroemer et al., 1997; Lu et al., 2010). Moreover, the biological function of Bcl-2 family proteins has been demonstrated to regulate mitochondrial-dependent apoptosis while balancing anti- and pro-apoptotic members to arbitrate life/death decisions. Therefore, the ratio of Bcl-2 to Bax is a pivotal factor that determines whether apoptosis will occur in the cells exposed to injurious chemicals (Cheng et al., 2007; Pradelli et al., 2010). Here, we found that MeHg is capable of inducing apoptotic cell death in Neuro-2a cells, which triggers MMP depolarization and cytochrome *c* release. Moreover, treatment with 3 μM MeHg significantly increased Bax and decreased Bcl-2 protein expression in Neuro-2a cells, and resulted in an increase in Bax/Bcl-2 ratio that might contribute to the promotion of MeHg-induced apoptosis. These MeHg-induced neuronal cell apoptotic responses could be prevented by the antioxidant NAC. Therefore, these results implicate that MeHg-induced oxidative stress-regulated Neuro-2a cell apoptosis is involved in the mitochondria-dependent apoptotic pathway.

MAPKs, including ERK1/2, JNK, and p38, play critical roles as mediators of cellular responses to extracellular stimuli, such as the proliferation, differentiation, survival, and death of nervous cells (Chang and Karin, 2001; Chen et al., 2009; Cowan and Storey, 2003). MAPK activation is also involved in apoptosis and may play a pivotal role in the progress of neurodegenerative diseases (Kim and Choi, 2010; Miloso et al., 2008). Some studies have indicated that oxidative stress is an important risk factor in the development of Alzheimer's disease via MAPK signaling activation and downstream-regulated apoptosis in neuronal cells exposed to many injurious agents (Marques et al., 2003; Puig et al., 2004). To

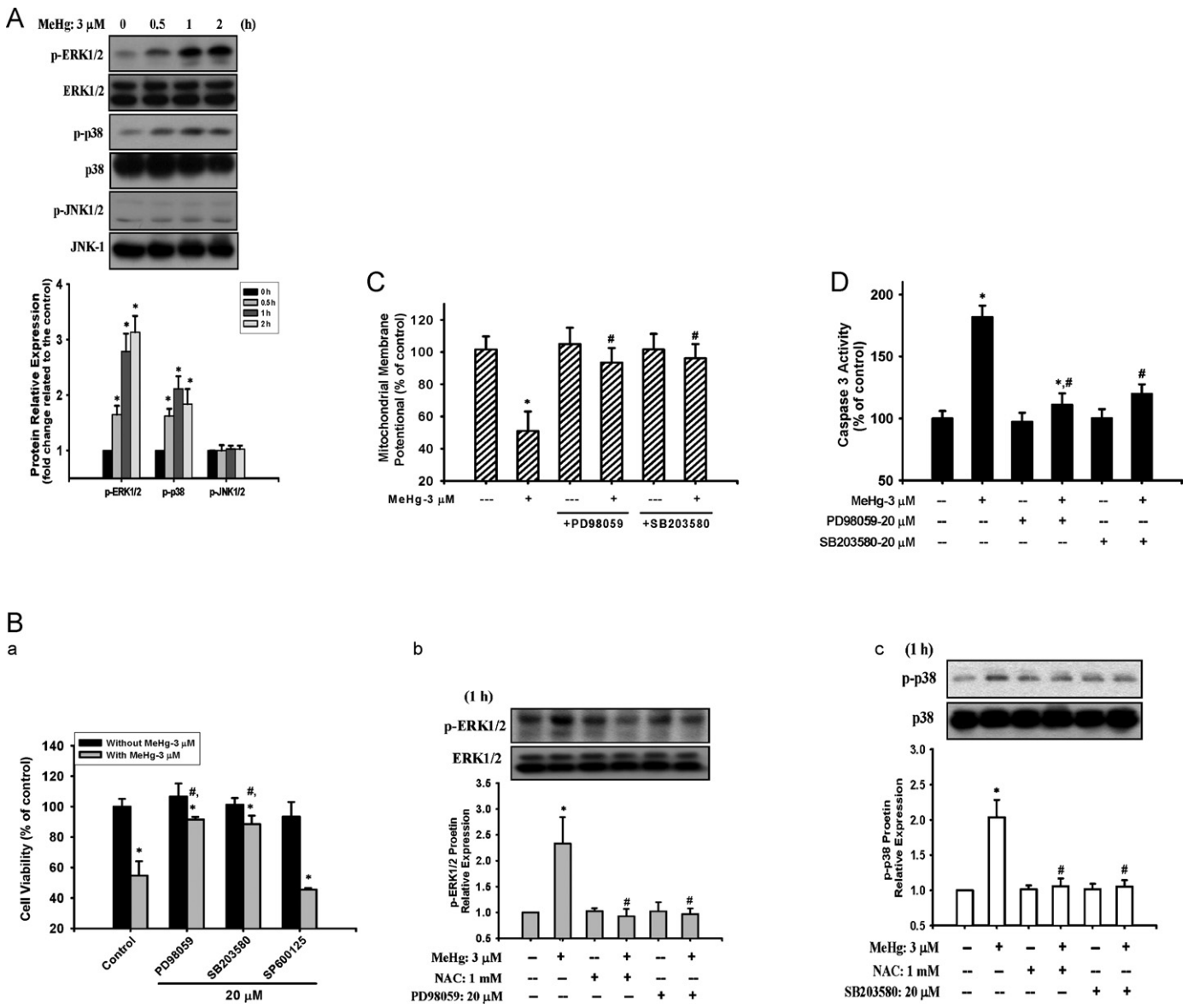

Fig. 6. MeHg-triggered ERK1/2- and p38-MAPK activation in Neuro-2a cells. (A) Cells were incubated with MeHg (3 μM) for 0.5–2 h, and ERK1/2- and p38-MAPK phosphorylation was analyzed by Western blotting. In addition, Neuro-2a cells were treated with MeHg (3 μM) in the absence or presence of EKR1/2 inhibitor (PD98059, 20 μM), p38 inhibitor (SB203580, 20 μM), or JNK inhibitor (SP600125, 20 μM). Cell viability was detected by MTT assay (B-a, for 24 h), the phosphorylation of ERK1/2- and p38-MAPK proteins were detected by Western blot analysis (B-b and c, for 1 h), MMP depolarization was determined by flow cytometry (C, for 24 h), and caspase-3 activity was measured by the CaspACE™ fluorometric activity assay kit (D, for 24 h) as described in Section 2. Results shown in A, B-b, and B-c are typical representatives of at least three independent experiments, the intensity of bands was analyzed by densitometry and expressed as fold changes relative to the control (mean ± S.D.). Data in B-a, C, and D are presented as mean ± S.D. for four independent experiments with triplicate determination. $^{*}p < 0.05$ as compared with vehicle control. $^{\#}p < 0.05$ as compared with MeHg alone.

our knowledge, however, a limited number of studies have investigated the role of MAPKs in MeHg-induced neuronal cell apoptosis. In the present study, we found that MeHg induced the activation of ERK1/2- and p38-MAPK, but not that of JNK, in Neuro-2a cells. Pretreatment of cells with the antioxidant NAC, specific ERK inhibitor PD98059, and p38 inhibitor SB203580, but not JNK inhibitor SP600125, attenuated MeHg-induced cytotoxicity and the phosphorylation levels of ERK1/2- and p38-MAPK protein expression. It also could significantly reverse MeHg-induced depolarization of MMP and the increase in caspase-3 activation by pretreatment with NAC and the specific ERK and p38 inhibitors. Moreover, the effects of MeHg-induced ERK1/2- and p38-MAPK activation were revealed in the cerebral cortex of mice exposed to MeHg (50 μg/kg/day, for 7 consecutive weeks), which could be prevented by NAC. Thus, these findings demonstrate that ROS-triggered ERK1/2- and p38-MAPK activated pathway mediate MeHg-induced neuronal cell apoptosis.

5. Conclusion

In conclusion, the present *in vivo* and *in vitro* results provide evidence that MeHg is capable of inducing neuronal degeneration and apoptosis, and more importantly reveal the molecular basis for its effects. This study has clearly demonstrated that MeHg-induced oxidative stress causes apoptosis in neuronal cells through ERK1/2- and p38-MAPK activation regulated mitochondrial dysfunction triggered PARP and caspase-9 activation, and involved in caspase-3/-7-mediated mechanism (Fig. 7). These observations further clarify the neurotoxic mechanisms of MeHg, and provide

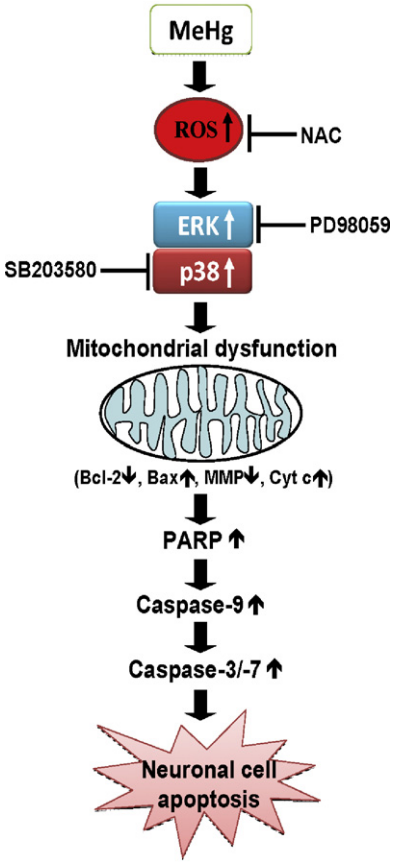

Fig. 7. Schematic diagram of the signal pathways involved in MeHg-induced neuron cell apoptosis. Proposed models show that MeHg causes neuron cell apoptosis through ROS-induced ERK1/2- and p38-MAPK activation regulated mitochondria-dependent signaling cascades.

beneficial evidence to suggest that MeHg-induced neurotoxicity may be an important risk factor for neurodegenerative diseases.

Conflict of interest statement

All authors declare that there are no conflicts of interest in this study.

Acknowledgments

This work was supported by research grants from the National Science Council of Taiwan (NSC 98-2314-B-039-015, NSC 98-2320-B-039-014-MY3, and NSC 99-2815-C-039-015-B), the China Medical University, Taichung, Taiwan (CMU99-N1-07-1 and CMU99-N1-07-2), and also supported in part by Taiwan Department of Health Clinical Trial and Research Center of Excellence (DOH100-TD-B-111-004).

Appendix A. Supplementary data

Supplementary data associated with this article can be found, in the online version, at doi:10.1016/j.toxlet.2011.04.013.

References

Amin-Zaki, L., Majeed, M.A., Greenwood, M.R., Elhassani, S.B., Clarkson, T.W., Doherty, R.A., 1981. Methylmercury poisoning in the Iraqi suckling infant: a longitudinal study over five years. J. Appl. Toxicol. 1, 210–214.

Aschner, M., Syversen, T., Souza, D.O., Rocha, J.B., Farina, M., 2007. Involvement of glutamate and reactive oxygen species in methylmercury neurotoxicity. Braz. J. Med. Biol. Res. 40, 285–291.

Barnham, K.J., Masters, C.L., Bush, A.I., 2004. Neurodegenerative diseases and oxidative stress. Nat. Rev. Drug Discov. 3, 205–214.

Bush, A.I., 2000. Metals and neuroscience. Curr. Opin. Chem. Biol. 4, 184–191.

Carvalho, M.C., Franco, J.L., Ghizoni, H., Kobus, K., Nazari, E.M., Rocha, J.B., Nogueira, C.W., Dafre, A.L., Muller, Y.M., Farina, M., 2007. Effects of 2,3-dimercapto-1-propanesulfonic acid (DMPS) on methylmercury-induced locomotor deficits and cerebellar toxicity in mice. Toxicology 239, 195–203.

Chang, L., Karin, M., 2001. Mammalian MAP kinase signalling cascades. Nature 410, 37–40.

Chen, X., Lan, X., Mo, S., Qin, J., Li, W., Liu, P., Han, Y., Pi, R., 2009. p38 and ERK, but not JNK, are involved in copper-induced apoptosis in cultured cerebellar granule neurons. Biochem. Biophys. Res. Commun. 379, 944–948.

Chen, Y.W., Huang, C.F., Tsai, K.S., Yang, R.S., Yen, C.C., Yang, C.Y., Lin-Shiau, S.Y., Liu, S.H., 2006. Methylmercury induces pancreatic beta-cell apoptosis and dysfunction. Chem. Res. Toxicol. 19, 1080–1085.

Chen, Y.W., Huang, C.F., Yang, C.Y., Yen, C.C., Tsai, K.S., Liu, S.H., 2010. Inorganic mercury causes pancreatic beta-cell death via the oxidative stress-induced apoptotic and necrotic pathways. Toxicol. Appl. Pharmacol. 243, 323–331.

Cheng, B., Yang, X., Hou, Z., Lin, X., Meng, H., Li, Z., Liu, S., 2007. D-beta-hydroxybutyrate inhibits the apoptosis of PC12 cells induced by 6-OHDA in relation to up-regulating the ratio of Bcl-2/Bax mRNA. Auton. Neurosci. 134, 38–44.

Chuu, J.J., Liu, S.H., Lin-Shiau, S.Y., 2007. Differential neurotoxic effects of methylmercury and mercuric sulfide in rats. Toxicol. Lett. 169, 109–120.

Clarkson, T.W., Magos, L., Myers, G.J., 2003. The toxicology of mercury—current exposures and clinical manifestations. N. Engl. J. Med. 349, 1731–1737.

Cowan, K.J., Storey, K.B., 2003. Mitogen-activated protein kinases: new signaling pathways functioning in cellular responses to environmental stress. J. Exp. Biol. 206, 1107–1115.

Cuello, S., Goya, L., Madrid, Y., Campuzano, S., Pedrero, M., Bravo, L., Camara, C., Ramos, S., 2010. Molecular mechanisms of methylmercury-induced cell death in human HepG2 cells. Food Chem. Toxicol. 48, 1405–1411.

Dare, E., Fetissov, S., Hokfelt, T., Hall, H., Ogren, S.O., Ceccatelli, S., 2003. Effects of prenatal exposure to methylmercury on dopamine-mediated locomotor activity and dopamine D2 receptor binding. Naunyn Schmiedebergs Arch. Pharmacol. 367, 500–508.

Dreiem, A., Gertz, C.C., Seegal, R.F., 2005. The effects of methylmercury on mitochondrial function and reactive oxygen species formation in rat striatal synaptosomes are age-dependent. Toxicol. Sci. 87, 156–162.

El-Najjar, N., Chatila, M., Moukadem, H., Vuorela, H., Ocker, M., Gandesiri, M., Schneider-Stock, R., Gali-Muhtasib, H., 2010. Reactive oxygen species mediate thymoquinone-induced apoptosis and activate ERK and JNK signaling. Apoptosis 15, 183–195.

Fujimura, M., Usuki, F., Sawada, M., Rostene, W., Godefroy, D., Takashima, A., 2009. Methylmercury exposure downregulates the expression of Racl and leads to neuritic degeneration and ultimately apoptosis in cerebrocortical neurons. Neurotoxicology 30, 16–22.

Garg, T.K., Chang, J.Y., 2006. Methylmercury causes oxidative stress and cytotoxicity in microglia: attenuation by 15-deoxy-delta 12,14-prostaglandin J2. J. Neuroimmunol. 171, 17–28.

Gerhardsson, L., Lundh, T., Minthon, L., Londos, E., 2008. Metal concentrations in plasma and cerebrospinal fluid in patients with Alzheimer's disease. Dement. Geriatr. Cogn. Disord. 25, 508–515.

Goulet, S., Dore, F.Y., Mirault, M.E., 2003. Neurobehavioral changes in mice chronically exposed to methylmercury during fetal and early postnatal development. Neurotoxicol. Teratol. 25, 335–347.

Grandjean, P., Weihe, P., Jorgensen, P.J., Clarkson, T., Cernichiari, E., Videro, T., 1992. Impact of maternal seafood diet on fetal exposure to mercury, selenium, and lead. Arch. Environ. Health 47, 185–195.

Harvilchuck, J.A., Carlson, G.P., 2009. Effect of multiple doses of styrene and R-styrene oxide on CC10, bax, and bcl-2 expression in isolated Clara cells of CD-1 mice. Toxicology 259, 149–152.

Hock, C., Drasch, G., Golombowski, S., Muller-Spahn, F., Willershausen-Zonnchen, B., Schwarz, P., Hock, U., Growdon, J.H., Nitsch, R.M., 1998. Increased blood mercury levels in patients with Alzheimer's disease. J. Neural. Transm. 105, 59–68, http://cmurdc.cmu.edu.tw/LA/index.php.

Hoijman, E., Rocha Viegas, L., Keller Sarmiento, M.I., Rosenstein, R.E., Pecci, A., 2004. Involvement of Bax protein in the prevention of glucocorticoid-induced thymocytes apoptosis by melatonin. Endocrinology 145, 418–425.

Huang, C.F., Hsu, C.J., Liu, S.H., Lin-Shiau, S.Y., 2008. Neurotoxicological mechanism of methylmercury induced by low-dose and long-term exposure in mice: oxidative stress and down-regulated Na+/K(+)-ATPase involved. Toxicol. Lett. 176, 188–197.

Huang, C.F., Liu, S.H., Hsu, C.J., Lin-Shiau, S.Y., 2011. Neurotoxicological effects of low-dose methylmercury and mercuric chloride in developing offspring mice. Toxicol. Lett. 201, 196–204.

Kalia, S., Bansal, M.P., 2009. Regulation of apoptosis by Caspases under oxidative stress conditions in mice testicular cells: in vitro molecular mechanism. Mol. Cell. Biochem. 322, 43–52.

Kim, E.K., Choi, E.J., 2010. Pathological roles of MAPK signaling pathways in human diseases. Biochim. Biophys. Acta 1802, 396–405.

Kim, S.H., Kim, S.C., Kho, Y.J., Kwak, S.W., Lee, H.G., You, S.K., Woo, J.H., Choi, Y.J., 2004. C2-ceramide as a cell death inducer in HC11 mouse mammary epithelial cells. Cancer Lett. 203, 191–197.

Kroemer, G., Zamzami, N., Susin, S.A., 1997. Mitochondrial control of apoptosis. Immunol. Today 18, 44–51.

Larkfors, L., Oskarsson, A., Sundberg, J., Ebendal, T., 1991. Methylmercury induced alterations in the nerve growth factor level in the developing brain. Brain Res. Dev. Brain Res. 62, 287–291.
Levesque, P.C., Atchison, W.D., 1991. Disruption of brain mitochondrial calcium sequestration by methylmercury. J. Pharmacol. Exp. Ther. 256, 236–242.
Li, P., Feng, X., Qiu, G., 2010. Methylmercury exposure and health effects from rice and fish consumption: a review. Int. J. Environ. Res. Public Health 7, 2666–2691.
Loh, K.P., Huang, S.H., De Silva, R., Tan, B.K., Zhu, Y.Z., 2006. Oxidative stress: apoptosis in neuronal injury. Curr. Alzheimer Res. 3, 327–337.
Lu, T.H., Chen, C.H., Lee, M.J., Ho, T.J., Leung, Y.M., Hung, D.Z., Yen, C.C., He, T.Y., Chen, Y.W., 2010. Methylmercury chloride induces alveolar type II epithelial cell damage through an oxidative stress-related mitochondrial cell death pathway. Toxicol. Lett. 194, 70–78.
Lu, T.H., Su, C.C., Chen, Y.W., Yang, C.Y., Wu, C.C., Hung, D.Z., Chen, C.H., Cheng, P.W., Liu, S.H., Huang, C.F., 2011. Arsenic induces pancreatic beta-cell apoptosis via the oxidative stress-regulated mitochondria-dependent and endoplasmic reticulum stress-triggered signaling pathways. Toxicol. Lett. 201, 15–26.
Maramba, N.P., Reyes, J.P., Francisco-Rivera, A.T., Panganiban, L.C., Dioquino, C., Dando, N., Timbang, R., Akagi, H., Castillo, M.T., Quitoriano, C., Afuang, M., Matsuyama, A., Eguchi, T., Fuchigami, Y., 2006. Environmental and human exposure assessment monitoring of communities near an abandoned mercury mine in the Philippines: a toxic legacy. J. Environ. Manage. 81, 135–145.
Marsh, D.O., 1987. Dose–response relationships in humans: methyl mercury epidemics in Japan and Iraq. In: Eccles, C.U., Annau, Z. (Eds.), The Toxicity of Methyl Mercury. The Johns Hopkins University Press, Baltimore, pp. 45–53.
Marques, C.A., Keil, U., Bonert, A., Steiner, B., Haass, C., Muller, W.E., Eckert, A., 2003. Neurotoxic mechanisms caused by the Alzheimer's disease-linked Swedish amyloid precursor protein mutation: oxidative stress, caspases, and the JNK pathway. J. Biol. Chem. 278, 28294–28302.
Martin, P., Pognonec, P., 2010. ERK and cell death: cadmium toxicity, sustained ERK activation and cell death. FEBS J. 277, 39–46.
Miloso, M., Scuteri, A., Foudah, D., Tredici, G., 2008. MAPKs as mediators of cell fate determination: an approach to neurodegenerative diseases. Curr. Med. Chem. 15, 538–548.
Min, H.Y., Kim, M.S., Jang, D.S., Park, E.J., Seo, E.K., Lee, S.K., 2009. Suppression of lipopolysaccharide-stimulated inducible nitric oxide synthase (iNOS) expression by a novel humulene derivative in macrophage cells. Int. Immunopharmacol. 9, 844–849.
Mutter, J., Naumann, J., Schneider, R., Walach, H., 2007. Mercury and Alzheimer's disease. Fortschr. Neurol. Psychiatr. 75, 528–538.
Navarro, R., Busnadiego, I., Ruiz-Larrea, M.B., Ruiz-Sanz, J.I., 2006. Superoxide anions are involved in doxorubicin-induced ERK activation in hepatocyte cultures. Ann. N. Y. Acad. Sci. 1090, 419–428.
Onishchenko, N., Tamm, C., Vahter, M., Hokfelt, T., Johnson, J.A., Johnson, D.A., Ceccatelli, S., 2007. Developmental exposure to methylmercury alters learning and induces depression-like behavior in male mice. Toxicol. Sci. 97, 428–437.
Pfaffl, M.W., Horgan, G.W., Dempfle, L., 2002. Relative expression software tool (REST) for group-wise comparison and statistical analysis of relative expression results in real-time PCR. Nucleic Acids Res. 30, e36.
Pradelli, L.A., Beneteau, M., Ricci, J.E., 2010. Mitochondrial control of caspase-dependent and -independent cell death. Cell Mol. Life Sci. 67, 1589–1597.
Puig, B., Gomez-Isla, T., Ribe, E., Cuadrado, M., Torrejon-Escribano, B., Dalfo, E., Ferrer, I., 2004. Expression of stress-activated kinases c-Jun N-terminal kinase (SAPK/JNK-P) and p38 kinase (p38-P), and tau hyperphosphorylation in neurites surrounding betaA plaques in APP Tg2576 mice. Neuropathol. Appl. Neurobiol. 30, 491–502.
Qiu, G., Feng, X., Li, P., Wang, S., Li, G., Shang, L., Fu, X., 2008. Methylmercury accumulation in rice (*Oryza sativa* L.) grown at abandoned mercury mines in Guizhou, China. J. Agric. Food Chem. 56, 2465–2468.
Rana, S.V., 2008. Metals and apoptosis: recent developments. J. Trace Elem. Med. Biol. 22, 262–284.
Rice, D., Barone Jr., S., 2000. Critical periods of vulnerability for the developing nervous system: evidence from humans and animal models. Environ. Health Perspect. 108 (Suppl. 3), 511–533.
Sarafian, T.A., 1999. Methylmercury-induced generation of free radicals: biological implications. Met. Ions Biol. Syst. 36, 415–444.
Shanker, G., Aschner, J.L., Syversen, T., Aschner, M., 2004. Free radical formation in cerebral cortical astrocytes in culture induced by methylmercury. Brain Res. Mol. Brain Res. 128, 48–57.
Sirois, J.E., Atchison, W.D., 2000. Methylmercury affects multiple subtypes of calcium channels in rat cerebellar granule cells. Toxicol. Appl. Pharmacol. 167, 1–11.
Tamm, C., Duckworth, J., Hermanson, O., Ceccatelli, S., 2006. High susceptibility of neural stem cells to methylmercury toxicity: effects on cell survival and neuronal differentiation. J. Neurochem. 97, 69–78.
Tofighi, R., Johansson, C., Goldoni, M., Ibrahim, W.N., Gogvadze, V., Mutti, A., Ceccatelli, S., 2011. Hippocampal neurons exposed to the environmental contaminants methylmercury and polychlorinated biphenyls undergo cell death via parallel activation of calpains and lysosomal proteases. Neurotox. Res. 19, 183–194.
U.S. EPA, 1997. Mercury Study Report to Congress, Vol. IV: An Assessment of Exposure to Mercury in the United States. Environmental Protection, Washington, DC, U.S. Available: http://www.epa.gov/ttn/oarpg/t3/reports/volume4.pdf (accessed 31 August 2009).
Yang, C., Kaushal, V., Haun, R.S., Seth, R., Shah, S.V., Kaushal, G.P., 2008. Transcriptional activation of caspase-6 and -7 genes by cisplatin-induced p53 and its functional significance in cisplatin nephrotoxicity. Cell Death Differ. 15, 530–544.
Yee, S., Choi, B.H., 1996. Oxidative stress in neurotoxic effects of methylmercury poisoning. Neurotoxicology 17, 17–26.
Yen, C.C., Lu, F.J., Huang, C.F., Chen, W.K., Liu, S.H., Lin-Shiau, S.Y., 2007. The diabetogenic effects of the combination of humic acid and arsenic: in vitro and in vivo studies. Toxicol. Lett. 172, 91–105.
Yin, Z., Milatovic, D., Aschner, J.L., Syversen, T., Rocha, J.B., Souza, D.O., Sidoryk, M., Albrecht, J., Aschner, M., 2007. Methylmercury induces oxidative injury, alterations in permeability and glutamine transport in cultured astrocytes. Brain Res. 1131, 1–10.